MR Spectroscopy in Gliomatosis Cerebri

Martin Bendszus, Monika Warmuth-Metz, Rüdiger Klein, Ralf Burger,
Christian Schichor, Jörg C. Tonn, and
Laszlo Solymosi

BACKGROUND AND PURPOSE: The diagnosis of gliomatosis cerebri with MR imaging is known to be difficult. We report on the value of MR spectroscopy in the diagnosis, grading, and biopsy planing in eight patients with histopathologically proved gliomatosis cerebri.

METHODS: Patients underwent MR imaging and MR spectroscopy (single-voxel point-resolved spectroscopy [PRESS] at 1500/135, and chemical-shift imaging [CSI] PRESS at 1500/135) before open (n = 4) or stereotactic (n = 4) biopsy. In six patients who underwent CSI, biopsy samples were taken from regions of maximally elevated levels of choline/*N*-acetylaspartate (Cho/NAA).

RESULTS: All patients showed elevated Cho/creatine (Cr) and Cho/NAA levels as well as varying degrees of decreased NAA/Cr ratios, which were most pronounced in the anaplastic lesions. In low-grade lesions, there was a maximum Cho/NAA ratio of 1.3, whereas in anaplastic tumors, the maximum Cho/NAA level was at least 2.5. Spectra in two patients with grade III lesions revealed a lactate peak; lactate and lipid signals were seen in two patients with grade IV lesions. Biopsy specimens from regions with maximally elevated levels of Cho/NAA showed dense infiltration of tumor cells.

CONCLUSION: MR spectroscopy might be used to classify gliomatosis cerebri as a stable or a progressive disease indicating its potential therapeutic relevance.

Gliomatosis cerebri is a rare brain tumor characterized by a diffuse neoplastic overgrowth of glial elements and extensive infiltration of at least two lobes (1). The neuronal architecture is usually preserved except in areas where the infiltration becomes very dense (2). Gliomatosis cerebri was first described by Nevin in 1938 (3) and, to date, fewer than 200 cases have been reported in the literature. MR imaging is the radiologic method of choice (4), but MR findings are often nonspecific and underestimate the extent of the lesion (5). Moreover, since the area of most extensive anaplasia determines the clinical course of the disease (6), it is important to define these targets before biopsy. The purpose of this study was to characterize the metabolic features of gliomatosis cerebri and to evaluate MR spectroscopy in the grading and biopsy planning of gliomatosis.

Methods

Eight patients (one woman and seven men, ages 10–67 years; mean age, 42 years) were examined on a 1.5-T MR scanner. MR imaging included T1-weighted sequences before and after injection of contrast material and T2-weighted sequences in all patients. Additionally, the fluid-attenuated inversion-recovery (FLAIR) sequence was applied in five patients. In all patients, the MR spectroscopy protocol consisted of single-voxel point-resolved spectroscopy (PRESS) with a voxel size of 15 to 25 mm³ and imaging parameters of 1500/135,270/128 (TR/TE/acquisitions) within the area of hyperintensity on T2-weighted images as well as in the margin of the lesion and, in cases with unilateral involvement, in the corresponding area of the contralateral, unaffected hemisphere. None of the patients who underwent only single-voxel spectroscopy had bilateral involvement. Additionally, chemical-shift imaging (CSI) with parameters of 1500/135/2 was used in six patients. The CSI voxel size was 7.5 × 7.5 × 15 mm. All data postprocessing was performed with software provided by the manufacturer. Spectral postprocessing included 4k zero-filling, gaussian apodization, Fourier transformation, water reference processing, frequency shift correction, and phase and baseline correction. Peak integral values were determined by a curve fit algorithm at 3.0 ppm for creatine (Cr), 3.2 ppm for choline-containing compounds (Cho), 1.35 for lactate, and 2.0 ppm for *N*-acetylaspartate (NAA). Peak integral values were normalized to the internal Cr peak.

Histopathologic diagnosis was confirmed by open (n = 4) or stereotactic (n = 4) biopsy. In six patients who underwent CSI, localizer images of the areas of maximally elevated Cho/NAA levels were given to the neurosurgeon, who performed a targeted biopsy of this area. These biopsies were not taken additionally to the requisite specimen for histopathologic di-

FIG 1. Case 4: 38-year-old woman with bifrontal hyperintensity and tumor spread via corpus callosum.

A, Axial T2-weighted spin-echo localizer image (1900/80).

B, Corresponding spectrum (CSI, PRESS, 1500/135, voxel size = 7.5 × 7.5 × 15 mm) shows a moderate increase in Cho/Cr and Cho/NAA and a decrease in NAA/Cr.
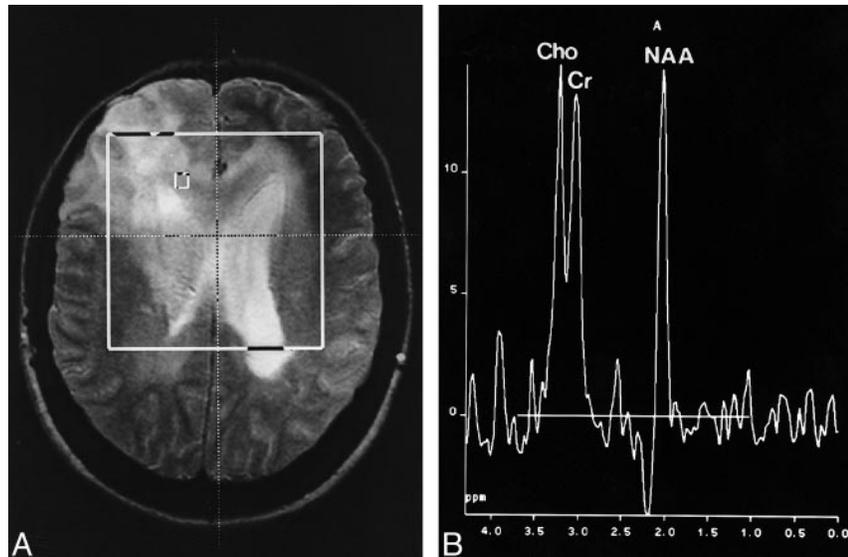
agnosis. In two patients who underwent single-voxel spectroscopy only, biopsy specimens were taken from brain tissue in the area corresponding to the voxel. A postoperative CT study was performed in all patients to ensure that the biopsy sample was taken from the intended location.

Representative Case Reports

Case 4

A 38-year-old woman presented with a short history of visual disturbance. The clinical examination revealed a visual acuity of 2/5 in the right eye. CT studies showed extensive areas of hypoattenuation in both hemispheres with little mass effect. MR images depicted diffuse T2 hyperintensities in both frontal and parietal lobes and a thickening of the optic chiasm (Fig 1A). There was no contrast enhancement after injection of gadopentetate dimeglumine. MR spectroscopy revealed a mild increase in the Cho/Cr and Cho/NAA ratios and a decrease

in the NAA/Cr ratio (Fig 1B). Lactate or lipids were not found. A targeted biopsy sample was taken from the area with the maximally elevated Cho/NAA level with a value of 1.1 and revealed a grade II lesion (lesion grades are in accordance with the World Health Organization [WHO] classification scheme).

Case 5

A 12-year-old boy presented after experiencing the first instance of a generalized seizure. The MR examination revealed extensive areas of hyperintensity on T2-weighted images affecting the cortex, white matter, and basal ganglia of the right hemisphere with little mass effect (Fig 2A). No enhancement was seen after injection of contrast material. Single-voxel MR spectroscopy and CSI revealed a marked increase of Cho/Cr and NAA/Cr and lactate in some parts of the lesion (Fig 2B).

FIG 2. Case 5: 12-year-old boy with seizure.

A, Axial T1-weighted localizer image (fast low-angle shot, 80/10) shows extensive hypointense infiltration of the right hemisphere with little mass effect.

B, Corresponding spectrum (CSI, PRESS, 1500/135, voxel size = 7.5 × 7.5 × 15 mm) shows a marked increase in Cho/Cr and Cho/NAA and a pronounced decrease in NAA/Cr. Moreover, there is a lactate doublet at 1.35 ppm.
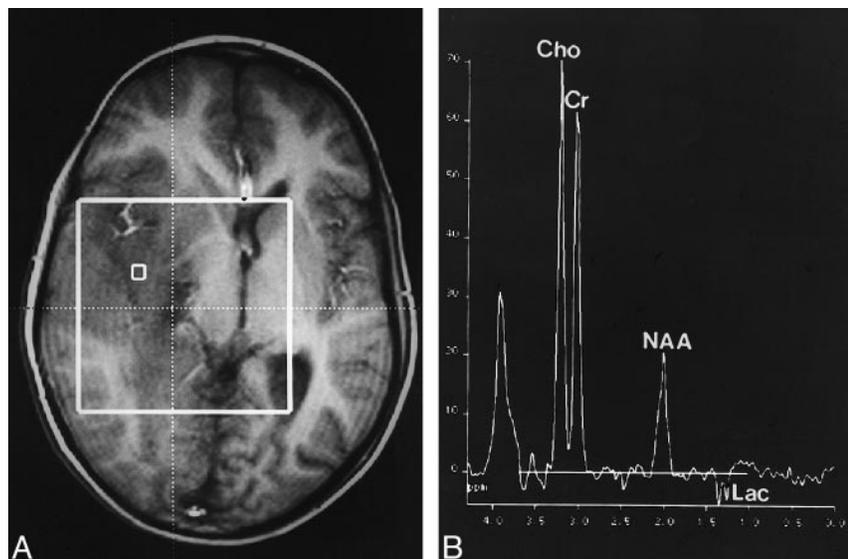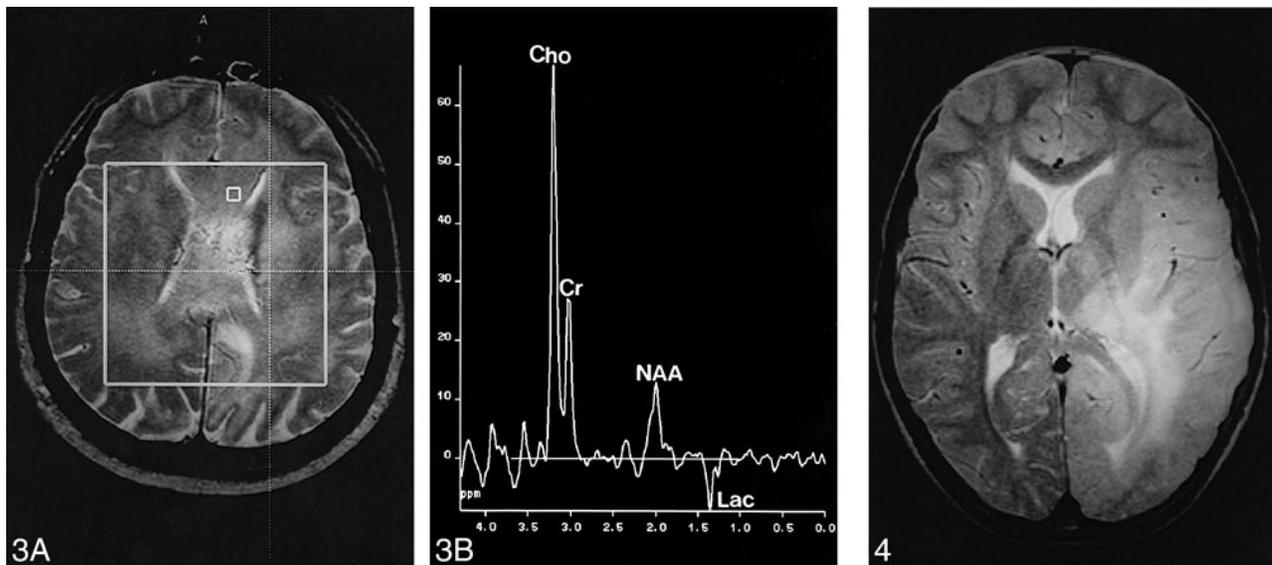
Fig 3. Case 8: 55-year-old man with diffuse involvement of both hemispheres.

A, Axial T2-weighted spin-echo localizer image (1900/80).

B, Corresponding spectrum. Stereotactic biopsy sample was taken from the denoted voxel, with a maximum Cho/NAA ratio of the lesion of 8.9 as well as a lactate doublet at 1.35 ppm. Histopathologic examination revealed a grade IV tumor. In other areas of the tumor there were lipid signals at 0.8 to 1.3 ppm (CSI, PRESS, 1500/135, voxel size = 7.5 × 7.5 × 15 mm).

Fig 4. Case 1: 10-year-old boy with seizure. Axial spin-echo T2-weighted image (1900/80) shows extensive hyperintensity of the left occipital, parietal, and temporal lobes, with infiltration of the thalamus and the insula. Both gray and white matter are affected, and there is little mass effect.

Targeted open biopsy was performed and, owing to the pronounced proliferative activity, the specimen was classified as a grade III lesion. The boy rapidly deteriorated, and focal neurologic signs developed. Despite radiotherapy, he died 20 months after the first symptoms appeared.

Case 8

A 55-year-old man presented with a short history of lack of drive and depression; a diagnosis of an endogenous depression was made. Because his symptoms rapidly worsened, a CT study was performed, which showed bifrontal areas of hypoattenuation. MR images exhibited an infiltration of both hemispheres, predominantly in the frontal lobes with involvement of the corpus callosum (Fig 3A). MR spectroscopy showed extensive elevation of the Cho/Cr and Cho/NAA levels and a decrease in the NAA/Cr ratio (Fig 3B). In some parts of the lesion, especially in the rostral corpus callosum, there were lipid signals at 0.8 to 1.3 ppm. A stereotactic biopsy was done in the area of the maximally elevated Cho/NAA level, with a value of 5.5 in the left frontal lobe. The histopathologic specimen was classified as a grade IV lesion.

Results

Clinical Findings

Clinical data are summarized in the Table. Considering the extent of tumor infiltration, patients had little symptomatology. In five patients, seizure

Data for eight patients with gliomatosis cerebri

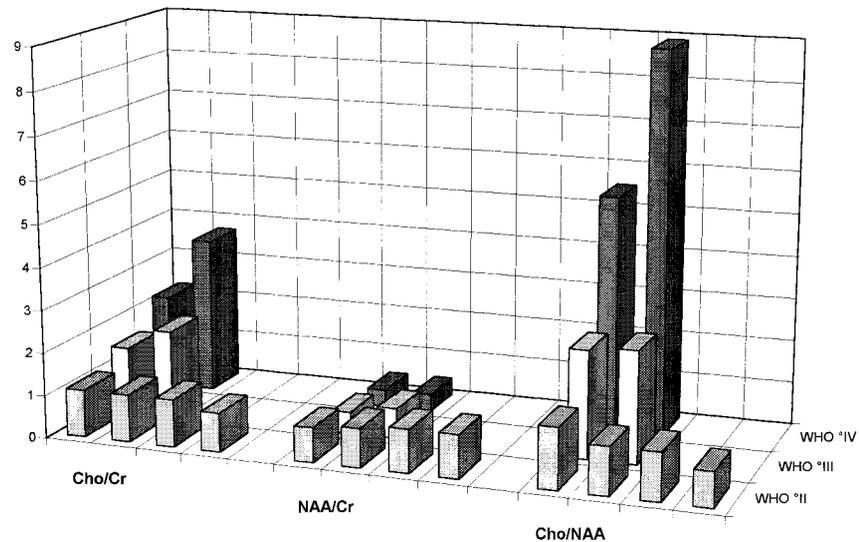| Case	Age (yr)/Sex	Clinical presentation	Lesion Grade*
1	10/M	Seizure	II
2	67/M	Seizure	II
3	30/M	Seizure	II
4	38/F	Visual loss	II
5	12/M	Seizure	III
6	63/M	Visual loss	III
7	62/M	Seizure	IV
8	55/M	Depression	IV

* Grades are in accordance with the classification scheme established by the World Health Organization.

was the initial neurologic symptom. Two patients (cases 4 and 6) had a short history of visual impairment due to infiltration of the chiasm and the optic nerves. One patient (case 8) presented with a short history of depression. The mean interval from symptom onset to diagnosis was 2 months (range, 1–9 months).

Imaging Findings

All patients had extensive areas of hyperintensity on T2-weighted images affecting at least two lobes (Fig 4), which appeared hypointense on T1-weighted images. The basal ganglia and the temporal and frontal lobes were affected in all patients. Additional infiltration of the parietal and occipital lobes was seen in five patients. Bilateral involvement was found in four patients. A typical finding in all pa-

tients was diffuse infiltration of the cortex with an enlargement of the cortical sulci and poor demarcation of the gray and white matter. Two patients had infiltration of the optic chiasm and the optic nerves. The brain stem and the cerebellum were not affected in any of our patients. Considering the extensive areas of signal abnormalities, there was only moderate mass effect. Two patients (cases 7 and 8) displayed patchy areas of contrast enhancement in the white matter on T1-weighted images. Areas of cortical or leptomeningeal enhancement were not found.

Spectroscopic Findings

All patients had elevated Cho/Cr and Cho/NAA ratios as well as decreased NAA/Cr ratios of varying degrees within the areas of hyperintensity on T2-weighted images (Figs 1–3). Anaplastic lesions exhibited markedly higher maximal Cho/Cr and Cho/NAA ratios and a lower NAA/Cr ratio (Fig 5). The difference between low- and high-grade tumors was most pronounced in the Cho/NAA ratio. Patients with a grade II lesion had a maximum NAA/Cho ratio of 1.3, whereas those with grade III (Fig 2) and grade IV (Fig 3) gliomatosis had a maximum value of at least 2.5, with no overlap between high- and low-grade lesions (Fig 5). The highest Cho/NAA ratio of 8.9 was found in a patient with grade IV gliomatosis. Lactate was found in all high-grade lesions (Figs 2 and 3). Lactate was differentiated from lipid signals by the inversion of the lactate doublet at 135 milliseconds. In two patients (cases 7 and 8, with grade IV tumors), lipid signals were found in some areas of the lesion. In patients who underwent CSI, there was a moderate elevation of Cho/Cr and a decrease of NAA/Cr in regions in the margin of the lesion that appeared normal on T2-weighted images.

Neuropathologic Findings

On slides stained with hematoxylin-eosin, the cortex and adjacent white matter showed a diffuse moderately dense infiltration of elongated tumor cells with little destruction of the parenchyma. Mitotic figures were infrequent. On the basis of cell density, cellular pleomorphism, frequency of mitosis, and proliferative activity, the diffusely infiltrating gliomas were categorized as grades II to III. Two lesions (in patients 7 and 8) showed, in addition to the diffusely infiltrating pattern, a few areas with the typical morphology of glioblastoma multiforme (grade IV). Targeted biopsy specimens taken from areas with maximally elevated Cho/NAA levels showed dense infiltration of neoplastic cells in all cases. There was a close relationship between anaplasia and extent of Cho/NAA increase, with a maximum ratio of 1.3 in grade II lesions and a minimum of 2.5 in grade III and IV tumors (Fig 5).

Discussion

Gliomatosis cerebri is characterized by a diffuse infiltration of neoplastic glial cells with preservation of neuronal architecture (3). In the latest WHO classification it is listed as a subgroup of neuroepithelial tumors of uncertain origin with involvement of at least two lobes without a cellular, centrally necrotic center (1). However, there is still debate as to whether gliomatosis cerebri is a histopathologic entity or just a heterogeneous group of gliomas characterized by the tendency of widespread infiltration (5, 7). Nevertheless, cytogenetic findings point at a distinct chromosomal alteration in gliomatosis cerebri as a distinguishing feature from astrocytomas (8).

The antemortem diagnosis of gliomatosis cerebri represents a differential diagnostic problem. The clinical findings are nonspecific and, in relation to

the extent of the lesion, quite moderate. CT findings are either normal or show areas of hypoattenuation with little mass effect (4, 9–11). MR imaging has become the radiologic method of choice, because it reveals a more extensive involvement of the CNS and subtle changes, such as involvement of the cortex or the basal ganglia (10–14). However, the changes on MR images are nonspecific and the differential diagnosis includes ischemia, multiple sclerosis, encephalitis, leukodystrophies, and subacute sclerosing panencephalitis (11, 15). There are many reports of a delayed antemortem diagnosis of gliomatosis cerebri (16–21). Different imaging techniques, such as positron emission tomography (22) or single-photon emission CT (16, 23), have revealed nonspecific changes in gliomatosis cerebri and thus do not contribute much to the differential diagnosis. MR spectroscopy provides a noninvasive biochemical assay of normal and pathologic brain tissue. A number of previous studies have reported increased Cho/Cr and Cho/NAA ratios in tumors as compared with normal brain tissue (24–27), supposedly caused by a decrease of NAA, reflecting replacement of neurons by neoplastic glial cells (28), and an increase of Cho, caused by an increased membrane turnover in tumors (29). This particular spectroscopic pattern of neoplastic brain lesions has been used to differentiate brain tumors (30) or to establish prognostic parameters (31). All our patients had similar spectra, with a pronounced increase in Cho/Cr and decrease in NAA/Cr, consistent with a neoplastic lesion. Yet a small percentage of nonneoplastic lesions may have a "neoplastic" spectral pattern (eg, elevated Cho and decreased NAA and Cr), like encephalitis, demyelination, or organizing hemorrhage (32), which underlines the need for histopathologic examination as the standard of reference.

The grading of gliomatosis is of great importance in prognosis and possibly in therapy. Even in the case of suspected gliomatosis cerebri, correct histopathologic diagnosis may be difficult on the basis of a focal biopsy specimen of a diffuse process (14, 23, 33). Biopsy planning based solely on MR findings may be misleading, because MR imaging is unreliable in the grading of gliomas (34), making it difficult to designate the target for the biopsy. The extent of Cho/Cr and Cho/NAA increases has been used as an aid in the grading of gliomas (35). In patients with low-grade lesions (WHO grade II), we observed a moderate Cho/NAA ratio increase of up to 1.3, whereas anaplastic lesions exhibited a distinctly higher Cho/NAA increase of at least 2.5, with the maximum value of 8.9 in a grade IV tumor. Thus, the area of maximum Cho/NAA increase may be used to assess the overall tumor grade and also to determine a target for open or stereotactic biopsy, as has already been described for low-grade astrocytomas (36). Apart from highly elevated Cho/Cr and Cho/NAA ratios, the occurrence of lipids in tumors is indicative of

a malignant lesion (37, 38). In all our patients with anaplastic gliomatosis (two with grade III tumors and two with grade IV tumors), there was a lactate doublet at 1.35 ppm that was not present in the low-grade lesions. The presence of lactate has been found to be a poor prognostic factor, independent of the histologic grade (39). This, however, is controversial, and even though lactate is more likely to be found in high-grade lesions, large studies have shown that lactate cannot be used as a reliable predictor of either malignancy or poor prognosis (37, 40).

Apart from being beneficial in the grading of gliomatosis cerebri, MR spectroscopy might reflect the true extent of neoplastic infiltration more accurately than MR imaging. Correlative studies have shown more extensive histopathologic involvement of the CNS than was expected on the basis of MR imaging findings (13, 15, 22, 41). In our patients, we observed elevated Cho/Cr and Cho/NAA ratios in the tumor margins that appeared normal on T2-weighted images. However, since we did not perform stereotactic biopsies of these regions, we do not have histopathologic proof of actual tumor invasion in these areas. In most of our patients we performed both single-voxel MR spectroscopy and CSI. In our view, single-voxel spectroscopy is suitable for a quick metabolic characterization of a lesion but it is unable to show spatial diversity. Moreover, single-voxel MR spectroscopy only shows the average of a large sample volume, which may include anaplastic and low-grade tumor portions as well as normal brain parenchyma. Therefore, lactate or lipid signals in small parts of the tumor may not be visible, and the maximum extent of the Cho increase and NAA loss will be underestimated. CSI is superior in spatial resolution, thus enabling the simultaneous characterization of smaller parts of the lesion, which is necessary for studying the lesion margins or defining targets for biopsy. Once the diagnosis of gliomatosis cerebri has been established, MR spectroscopy can also be used for follow-up examinations. The natural course is quite variable, with a duration between 25 days and 22 years (8, 42). Especially in low-grade lesions, radiotherapy is of questionable benefit and of potential harm (14, 43), even though some recent publications have reported a benefit from radiotherapy in patients with gliomatosis cerebri (6, 44). It has been shown that increased Cho/Cr and Cho/NAA levels and the appearance of lipids indicate malignant progression of a brain tumor (24). Thus, MR spectroscopy might be used to classify gliomatosis cerebri as a stable or a progressive disease with potential therapeutic relevance.

References

1. Kleihues P, Burger PC, Scheithauer PW. **The new WHO classification of brain tumors.** *Brain Pathol* 1993;3:255–268
2. Couch JR, Weiss SA. **Gliomatosis cerebri.** *Neurology* 1974;24:504–511
3. Nevin S. **Gliomatosis cerebri.** *Brain* 1938;61:170–191

4. Carpio-O'Donovan R, Korah I, Salazar A, Melacon D. **Gliomatosis cerebri.** *Radiology* 1996;198:831–835

5. Burger PC, Scheithauer BW. *Atlas of Tumor Pathology: Tumors of the Central Nervous System.* Washington, DC: Armed Forces Institute of Pathology; 1994: 3rd series, fasc. 10

6. Cozad SC, Townsend P, Morantz RA, Jenny AB, Kepes JJ, Smalley SR. **Gliomatosis cerebri: results with radiation therapy.** *Cancer* 1996;78:1789–1793

7. Fallentin E, Skriver E, Herning, M, Broholm H. **Gliomatosis cerebri: an appropriate diagnosis?** *Acta Radiol* 1997;38:381–390

8. Hecht BK, Turc-Carel C, Chatel M, et al. **Chromosomes in gliomatosis cerebri.** *Genes Chromosomes Cancer* 1995;14:149–153

9. Artigas J, Cervos-Navarro J, Iglesias JR, Ebhard G. **Gliomatosis cerebri: clinical and histological findings.** *Clin Neuropathol* 1985;4:135–148

10. Geremia GK, Wollmann R, Foust R. **Computed tomography of gliomatosis cerebri.** *J Comput Assist Tomogr* 1988;12:698–701

11. Shin YM, Chang KH, Han MH, et al. **Gliomatosis cerebri: comparison of MR and CT features.** *AJR Am J Roentgenol* 1993;161:859–862

12. Spagnoli MV, Grossmann RI, Packer RJ, et al. **Magnetic resonance imaging determination of gliomatosis cerebri.** *Neuroradiology* 1987;29:15–18

13. Koslow SA, Claassen D, Hirsch WL, Jungreis CA. **Gliomatosis cerebri: a case report with autopsy correlation.** *Neuroradiology* 1992;34:331–333

14. Yanaka K, Kamzaki T, Kobayashi E, Matsueda K, Yoshihiko Y, Nose T. **MR-imaging of diffuse glioma.** *AJNR Am J Neuroradiol* 1992;13:349–351

15. Felsberg GJ, Silver SA, Brown MT, Tien RD. **Gliomatosis cerebri: radiologic-pathologic correlation.** *AJNR Am J Neuroradiol* 1994;15:1745–1751

16. Phhtinen J, Pääkkö E. **A difficult diagnosis of gliomatosis cerebri.** *Neuroradiology* 1996;38:444–448

17. Nishioka H, Ito H, Miki T. **Difficulties in the antemortem diagnosis of gliomatosis cerebri: report of a case with diffuse increase of gemistocyte-like cells, mimicking reactive gliosis.** *Br J Neurosurg* 1996;10:103–107

18. di Trapani G, Sabatelli M, Carnevale A, Colosimo A, Mignogna T, Tonali P. **Gliomatosis cerebri: report of an atypical case.** *Clin Neuropathol* 1995;14:13–18

19. Iglesias A, Garcia M, San Millan J, Villanueva C, Fraile G, Serrano M. **Gliomatosis cerebri mimicking a metastatic breast cancer: fatal outcome.** *J Neurooncol* 1997;32:175–178

20. Önal C, Bayindir C, Siraneci R, et al. **A serial CT scan and MRI verification of diffuse cerebrospinal gliomatosis: a case report with stereotactic diagnosis and radiological confirmation.** *Pediatr Neurosurg* 1996;25:94–99

21. Schoenen J, De Leval L, Reznik M. **Gliomatosis cerebri: clinical, radiological and pathological report of a case with stroke-like onset.** *Acta Neurol Belg* 1996;96:294–300

22. Dexter MA, Parker GD, Besser M, Ell J, Fulham MJ. **MR and positron emission tomography with fludeoxyglucose F 18 in gliomatosis cerebri.** *AJNR Am J Neuroradiol* 1995;15:1507–1510

23. Ross IB, Robitaille Y, Villemure JG, Tampieri D. **Diagnosis and management of gliomatosis cerebri: recent trends.** *Surg Neurol* 1991;36:431–440

24. Raman R, Sobering GS, Franck JA, Dwyer AJ, Alger JR, DiChiro G. **Mapping of human brain tumor metabolites with proton MR spectroscopic imaging: clinical relevance.** *Radiology* 1992;185:675–686

25. Kugel H, Heindel W, Ernestus R, Bunke J, Du Mesnil R, Friedmann G. **Human brain tumors: spectral patterns detected with localized 1-H MR-spectroscopy.** *Radiology* 1992;183:701–709

26. Ott D, Hennig J, Ernst T. **Human brain tumors: assessment with in vivo proton MR spectroscopy.** *Radiology* 1993;186:745–752

27. Houkin K, Kamada K, Sawamura Y, Iwasaki Y, Abe H, Kashiwaba T. **Proton magnetic resonance spectroscopy (1H-MRS) for the evaluation of treatment of brain tumors.** *Neuroradiology* 1995;37:99–103

28. Bruhn H, Michaelis T, Merboldt KD. **On the interpretation of proton NMR spectra from brain tumors in vivo and in vitro.** *NMR Biomed* 1992;5:253–258

29. Bruhn H, Frahm J, Gyngell M, et al. **Noninvasive differentiation of tumors with use of localized H-1 MR spectroscopy in vivo: initial experience in patients with cerebral tumors.** *Radiology* 1989;172:541–548

30. Preul MC, Caramanos Z, Collins DL, et al. **Accurate, noninvasive diagnosis of human brain tumors by using proton magnetic resonance spectroscopy.** *Nat Med* 1996;2:323–325

31. Girad N, Wang ZJ, Erbetta A, et al. **Prognostic value of proton MR spectroscopy of cerebral hemisphere tumors in children.** *Neuroradiology* 1998;40:121–125

32. Krouwer HGJ, Kim TA, Prost RW, et al. **Single-voxel proton MR spectroscopy of nonneoplastic brain lesions suggestive of a neoplasm.** *AJNR Am J Neuroradiol* 1998;19:1695–1703

33. Schober R, Mai JK, Volk B, Wechsler W. **Gliomatosis cerebri: bioptical approach and neuropathological verification.** *Acta Neurochir (Wien)* 1991;113:131–137

34. Kondziolka D, Lunsford LD, Martinez AJ. **Unreliability of contemporary neurodiagnostic imaging in evaluating suspected adult supratentorial (low grade) astrocytoma.** *J Neurosurg* 1993;79:533–536

35. Poptani H, Gupta RK, Pandey R, Jain VK, Chhabra DK. **Characterization of intracranial mass lesions with in vivo MR spectroscopy.** *AJNR Am J Neuroradiol* 1995;16:1593–1603

36. Go KG, Keuter EJW, Kamman RL, et al. **Contribution of magnetic resonance spectroscopic imaging and L-[1-^{11}C] tyrosine positron emission tomography to localization of cerebral gliomas for biopsies.** *Neurosurgery* 1994;34:994–1002

37. Negendank WG, Sauter R, Brown TR, et al. **Proton magnetic resonance spectroscopy in patients with glial tumors: a multicenter study.** *J Neurosurg* 1996;83:449–458

38. Kuesel AC, Sutherland GR, Halliday W, Smith ICP. **^{1}H MRS of high grade astrocytomas: mobile lipid accumulation in necrotic tissue.** *NMR Biomed* 1994;7:149–155

39. Negendank W. **Studies of human brain tumors by MRS: a review.** *NMR Biomed* 1992;5:303–324

40. Tien RD, Lai PH, Smith JS, Lazeyras F. **Single-voxel proton spectroscopy exam (PROBE/SV) in patients with primary brain tumors.** *AJR Am J Roentgenol* 1996;167:201–209

41. Rippe DJ, Boyko OB, Fuller GN, Friedman HS, Oakes WJ, Schold SC. **Gadopentate-dimeglumine-enhanced MR imaging of gliomatosis cerebri: appearance mimicking leptomeningeal tumor dissemination.** *AJNR Am J Neuroradiol* 1992;13:349–351

42. Blumbergs PC, Chin DF, Hallpike JF. **Diffuse infiltrating astrocytoma (gliomatosis cerebri) with twenty-two-year history.** *Clin Exp Neurol* 1983;19:94–101

43. Ross IB, Robitaille Y, Villemure JG, Tampieri D. **Diagnosis and management of gliomatosis cerebri: recent trends.** *Surg Neurol* 1991;36:431–440

44. Kim DG, Yang HJ, Park IA, et al. **Gliomatosis cerebri: clinical features, treatment and prognosis.** *Acta Neurochir* 1998;140:755–762